Effect of filler particle shape on plastic-elastic mechanical behavior of high density poly(ethylene)/mica and poly(ethylene)/wollastonite composites

Lapčík, Lubomír; Maňas, David; Lapčíková, Barbora; Vašina, Martin; Staněk, Michal; Čépe, Klára; Vlček, Jakub; Waters, Kristian E.; Greenwood, Richard W.; Rowson, Neil A.

DOI:
10.1016/j.compositesb.2017.12.035

Document Version
Peer reviewed version

Citation for published version (Harvard):
Lapčík, L, Maňas, D, Lapčíková, B, Vašina, M, Staněk, M, Čépe, K, Vlček, J, Waters, KE, Greenwood, RW & Rowson, NA 2018, 'Effect of filler particle shape on plastic-elastic mechanical behavior of high density poly(ethylene)/mica and poly(ethylene)/wollastonite composites', *Composites Part B: Engineering*, vol. 141, pp. 92-99. https://doi.org/10.1016/j.compositesb.2017.12.035

Effect of filler particle shape on plastic-elastic mechanical behavior of high density poly(ethylene)/mica and poly(ethylene)/wollastonite composites

Lubomír Lapčík[*1,2], David Maňas[†1], Barbora Lapčíková[1,2], Martin Vašina[1,3], Michal Staněk[1], Klára Čépe[2], Jakub Vlček[2], Kristian E. Waters[4], Richard W. Greenwood[5], Neil A. Rowson[5]

[1]Tomas Bata University in Zlin, Faculty of Technology, Nam. T.G. Masaryka 275, 760 01 Zlin, Czech Republic

[2]Regional Centre of Advanced Technologies and Materials, Department of Physical Chemistry, Faculty of Science, Palacky University, 17. Listopadu 12, 771 46 Olomouc, Czech Republic

[3]VŠB-Technical University of Ostrava, Department of Hydromechanics and Hydraulic Equipment, Faculty of Mechanical Engineering, 17. Listopadu 15/2172, 708 33 Ostrava-Poruba, Czech Republic

[4]Department of Mining and Materials Engineering, McGill University, M.H. Wong Building, 3610 University Street, Montreal, H3A 0C5, Québec, Canada

[5]School of Chemical Engineering, University of Birmingham, Edgbaston, Birmingham, B15 2TT, UK

[*]Corresponding author: L. Lapčík, Regional Centre of Advanced Technologies and Materials, Department of Physical Chemistry, Faculty of Science, Palacky University, 17. Listopadu 12, 771 46 Olomouc, Czech Republic. Email: lapcikl@seznam.cz (L. Lapčík).

[†]Deceased 16.9.2017.

ABSTRACT

It was found in this study that both fillers (mica and wollastonite) trigger an increase in Young´s modulus of elasticity with increasing filler concentration in a HDPE composites matrix. In the case of HDPE/mica the same improvement was also found for the upper yield point vs. filler concentration dependencies indicating higher stiffness. However, for the HDPE/wollastonite composites the opposite trend was observed, i.e. a decrease of the upper yield point and strain at break. These findings were also confirmed by mechanical vibration damping testing where there was found a more intense shift of the first resonance frequency peak position to higher frequencies with increasing filler concentrations for HDPE/mica in comparison to HDPE/wollastonite composites. Both composites exhibited decreasing strain at break with increasing filler concentration indicating a more brittle mechanical behavior in comparison to the virgin HDPE polymer matrix. However, for HDPE/wollastonite composites at 5 w. % filler concentration a 15 % increase in the magnitude of the strain at break was found indicating an increase in ductility at 50 mm/min deformation rate. Fracture toughness measurements show, that both studied fillers function as the stress concentrators in the HDPE polymer matrix, which was reflected in the exponentially decreasing dependencies of the fracture toughness vs. filler concentrations. SEM analysis of the fracture surfaces show typical elongation bands of high plasticity deformation regions characteristic of typical shearing bands, interpenetrated with cavities created around filler particles. Thermal analysis data showed for HDPE/mica a strong increase of the crystallinity with increasing filler concentration, however in the case of HDPE/wollastonite the opposite effect of a higher amorphous polymer phase content was found.

Keywords: HDPE; Mica; Wollastonite; Impact testing; Tensile testing; Vibration damping; SEM; Thermal analysis.

1. Introduction

At the present time, the engineering and materials science interests in automotive and aerospace industries are focused on the development and application of composite structures in construction of complex products exhibiting specific physico-chemical and material properties [1]. One of the aims is to obtain the elasto-mechanical behavior of complex structures to be capable to withstand the applied external mechanical loads without damage of the individual structural components. Traditional reinforcing fillers such as glass, carbon [2-4], boron fibers, calcium carbonate [5], carbon black, titanium dioxide, kaolin [6], silicon dioxide, wollastonite [7] and mica particles were added to polyolefin matrices to improve their rigidity, high temperature resistance, toughness etc. [8-12]. Furthermore, there were numerous applications of novel fillers in the production of polyethylene based composites, such as carbon nanotubes [13], cellulose fibers of different nature [14-16], metal powders [17,18], peat ash [19] etc. Thermoplastics, such as poly(ethylene) (PE) can offer useful mechanical, chemical, electrical properties, with low density, high formability and the ability to be recycled. Due to its low price per unit volume and its unique physico-chemical properties it is therefore, the world's number one per volume most used thermoplastic [6]. This semi-crystalline polymer can be classified according its density and divided into four groups: high density polyethylene (HDPE), low density polyethylene (LDPE), linear low density polyethylene (LLDPE), and very low density polyethylene (VLDPE). In general, semi-crystalline polymers such as HDPE are regarded as a three-phase continuum composed of an amorphous phase, a crystalline phase, and an inter-phase. The crystalline skeleton is formed by mutually connected spherulites, each of them consist of a number of crystalline lamellae with an amorphous phase located in between the crystallites and lamellae [5,20-22]. Different crystalline morphologies, such as spherulites, cylindrites, shis-kebab and fibrous

crystal can be obtained with variety processing conditions [23,24]. It was found, that the type and size of the filler particles has a strong effect on the HDPE crystallization kinetics and melting behavior [25,26] as well. However, no changes in the thermal oxidation mechanism of HDPE based composites filled with different inorganic fillers (e.g. mica, wollastonite, kaolin, talc or diatomite) were found [27]. In general, stress transfer in composite matrices is affected by structural, morphological and surface properties of the filler/matrix interface [11]. It is well known, that the polymer/filler interface quality performance is essential for excellent overall composite system material/mechanical properties. The exact adjustment of the polymer matrix modulus and adhesive bond strength is vital for the final synergistic increase in mechanical strength of the resulting composite system [28]. In most cases, silane coupling agents were used to create covalent bonds between filler particles and the polymer matrix [6,28-30]. In a paper [31] a prediction of the complex modulus of elasticity was studied at various strain rates by means of dynamic mechanical analysis. There was found a linear viscoelastic response to a given strain history. The paper of Xiang et al. [12] was studying DMA (Dynamic Mechanical Analysis) of HDPE/mica composites in a single cantilever mode at a frequency of 1 Hz. Tested composites were prepared by a dynamic packing injection molding (DPIM) technique allowing proper control of the central and skin layers of the prepared testing articles. They proposed the effect of the additional mica delamination induced by the injection flow and its orientation within the flow direction, allowing thus HDPE macromolecules melted matrix its intercalation in between galleries of mica layers under applied shear conditions. As a result, an increased storage modulus was found reflecting higher stiffness of the DPIM prepared HDPE/mica composite materials.

In this study, the mechanical properties of composites prepared from commercially available filler materials of mica (muscovite type) and wollastonite in HDPE matrix were investigated. Mica belongs to a group of silicate minerals, with the most common being muscovite

($KAl_2(AlSi_3O_{10})(OH)_2$). Micas are used as a filler in insulators, condensers, plastics, cosmetics and paints. Micas are sheet silicate minerals whose TOT-type (tetrahedral-octahedral-tetrahedral) sheets are made of two tetrahedral layers sandwiching an octahedral layer. The tetrahedral layers consist of a hexagonal pavement of tetrahedra $(SiO_4)^{4-}$ in which each tetrahedron shares three apexes with the neighboring tetrahedra: the chemical composition of such layers is $(Si_4O_{10})^{4-}$. In each sheet, the tetrahedra of the upper tetrahedral layer point downwards, and the ones of the lower tetrahedral sheet point upwards [32]. The most prominent characteristic of mica is nearly a perfect basal cleavage. Wollastonite is a calcium silicate ($CaSiO_3$) industrial mineral, which is commonly used as a filler in paints and plastics [33,34]. It is also used in the construction industry as a substitute for asbestos; ceramic applications including ceramic glazes and bodies; in metallurgical applications wollastonite is commonly added to formulated powders for steel casting and welding. It is the only naturally occurring needle-shaped crystal, and the shape is an important economic aspect of wollastonite, with highly acicular samples being most expensive. There are three polymorphs: triclinic pseudowollastonite of very high temperature (above 1120°C), monoclinic wollastonite-2M and triclinic wollastonite-Tc at lower temperatures. The usual form of wollastonite is the triclinic form.

As mentioned above, the reinforcing platelet shaped silicates in polymeric materials have been widely used due to their high aspect ratio, the effect of two-dimensional reinforcing as well as the overall materials cost reducing effect. However, the majority of the studies were performed in the static mechanical tensile testing configurations. Hence the better knowledge of the dynamic-mechanical performance at a wide frequency range is missing. This paper aims to study the effect of planar shape mica and prism shape wollastonite filler particles in HDPE polymer composites, specially investigating the mechanical properties (both static and

dynamic in a frequency range of 2 to 3200 Hz), and the thermal and fracture mechanical behaviors. This will be combined with SEM analysis.

2. Materials and processing

High density poly(ethylene) (HDPE) type 25055E (The Dow Chemical Company, USA) was purchased in the form of white pellets (lot. No. 1I19091333). As filler particles the inorganic minerals muscovite mica (Imerys, Kings Mountains, USA) (specific surface area of 9.7 m^2/g, d_{50} of 17 µm, aspect ratio of 1.7) and wollastonite type VANSIL W-10 (Vanderbilt Minerals, Norwalk, USA) (specific surface area of 0.5 m^2/g, d_{50} of 49 µm, aspect ratio of 13.5) were used. There were prepared 250 composites samples of each filler type (dog bone shape for tensile testing, Charpy´s pendulum and vibrator testing) of virgin HDPE and 5, 10 and 15 w.% of inorganic filler concentrations of HDPE/mica and HDPE/wollastonite composites. Composite samples were made using the injection molding technique on the injection molding machine Arburg Allrounder 420C (Germany). Parameters for the injection molding machine: 1 × 40 mm diameter rotating screw, length 800 mm (L/D = 20). The processing temperature ranging from 190 to 220 °C, the mold temperature was kept at 30 °C, the injection pressure was 60 MPa, and the injection rate was 20 mm/s, injection cycle time was 45 s, holding pressure time was 15 s. Studied melted matrices were filled at the central part of the mold during injection molding process, thus enhancing flux of the material in the direction of the longer side of the dog bone testing articles. There were found parallel orientations of the filler particles in the final composite testing articles by SEM analysis. (For the visualization of the flux of the polymer matrix/filler melt in the mold see Appendix A. Supplementary data). As a feed material for injection molding granules prepared by melt blending of the polymer resin and the mineral filler were used. The latter granules were prepared by means of extrusion technique on extrusion machine LABTECH engineering

model LTE20-40 Scientific (Thailand). Parameters of the extrusion machine were: 2 × 20 mm diameter co-rotating screws, length 800 mm (*L/D* = 40), extrusion rate 200 rpm, feeding rate 30 rpm. For the virgin HDPE processing temperature profile ranged from 136 to 172 °C. The mica and wollastonite filled HDPE samples temperature profiles ranged from 140 to 174 °C.

3. Methods

3.1. Scanning Electron Microscopy

Scanning electron microscopy (SEM) was used to determine the shape and size of the studied mineral composite filler particles. SEM images were captured using a Scanning Electron Microscope Hitachi SU 6600 (Japan). The source of the electrons is Schottky cathode. This microscope has the resolution in secondary electron mode (SE) 1.3 nm and in back scattered electrons (BSE) 3 nm. For these images, the secondary electron mode (SE) and an accelerating voltage of 5 kV (Fig. 1) or 1 kV (Fig. 2) were used. The distance between sample and detector was 6 mm. Studied materials were placed on double sided carbon tape on aluminum holder. All samples were metallized by gold with the thickness of 15 nm on sputter coater Quantum Q150T, LOT-Quantum Design (Germany) prior to the SEM measurements. All captured SEM images were taken from the surface fractured sections located at the central parts of the testing articles as obtained during uniaxial tensile testing or Charpy´s pendulum impact testing.

3.2. Thermal Analysis

Thermogravimetry (TG) and differential thermal analysis (DTA) experiments were performed on a simultaneous TG-DTA apparatus (Shimadzu DTG 60, Japan). Throughout the experiment, the sample temperature and weight loss were continuously monitored. The measurements were performed at a heat flow rate of 10 °C/min in a dynamic nitrogen

atmosphere (50 ml/min) over the temperature range from 30 °C to 550 °C. The crystallinity X_C of the composites was calculated according to the formula (1) [35,36]:

$$X_C = \frac{\Delta H_m}{(1-c) \times \Delta H^*} \times 100 \quad (1)$$

where c is the filler concentration (as mass fraction), ΔH_m is melting enthalpy of the tested sample, ΔH^* is the melting enthalpy of 100% crystallinity HDPE (293 J/g) [35]. Each experiment was repeated five times. Tested material was taken from the injection molded samples from the central part of the dog bone shape testing articles used for uniaxial tensile testing experiments.

3.3. Uniaxial tensile testing

For tensile testing of injection-molded specimens a Zwick 1456 multipurpose tester (Germany) and Universal Testing Machine Autograph AGS-X Shimadzu (Japan) equipped with the Compact Thermostatic Chamber TCE Series were used. The measurements were performed according to the CSN EN ISO 527-1 and CSN EN ISO 527-2 standards with the tested specimen gauge length of 80 mm. The specimens were strained at room temperature up to break at a test speeds of 50, 100 and 150 mm/min. From the stress–strain dependences, strength at break, Young´s modulus and strain at break were calculated. Each experiment was repeated 10 × at the ambient temperature of 22 °C and average values and standard errors were calculated.

3.4. Charpy impact testing

Impact tests were performed on Zwick 513 Pendulum Impact Tester (Germany) according to the CSN EN ISO 179-2 standard with the drop energy of 25 J. Each experiment was repeated 10 times.

3.5. Mechanical vibration damping testing

In the case of harmonic vibration, the transfer damping function D (dB) is given by the equation [5,37]:

$$D = 20 \cdot log \frac{a_1}{a_2} \quad (2)$$

where a_1 is the acceleration amplitude on the input side of the tested material, and a_2 is the acceleration amplitude on the output side of the tested material. The damping properties of the investigated HDPE composites were obtained by the forced oscillation method [37-39]. The transfer damping function was experimentally measured using a BK 4810 vibrator device in combination with a BK 3560-B-030 three-channel signal pulse multi-analyzer and a BK 2706 power amplifier operating over a frequency range of 2-3200 Hz. Sine waves were generated by the vibrator device in this case. The acceleration amplitudes on the input and output sides of the investigated specimens were recorded by BK 4393 accelerometers (Brüel & Kjær, Denmark). Measurements of the transfer damping function were performed for three different mass loads (i.e., 0 g, 85 g and 500 g) located on the upper side of the periodically loaded tested materials. The tested block article dimensions were (60 × 60 × 4) mm (length × width × thickness). Each experiment was repeated 10 times at the ambient temperature of 22 °C.

4. Results and discussion

In Fig. 1 representative SEM analysis results are shown, indicating the planar random shape of mica filler particles of about 30 μm rectangular size and of 1.7 μm thickness and the prism shape of wollastonite filler particles of about (150 × 20 × 10) μm size (length × width × thickness). Plastically deformed fibrils [5,6,40-42] typical for HDPE tensile behavior (Fig. 2F), known as the deformation to shear yielding, were observed also for both the HDPE/mica (Fig. 2B), as well as in part for HDPE/wollastonite composites (Fig. 2D). There was a relatively weak adhesion between the filler and the matrix after stress load in both studied composites, characteristic with the occurrence of the small cavities around individual particles as observed after uniaxial tensile testing (Figs. 2B and 2D). Furthermore, in contrary to HDPE/mica composites, there were found small crazes oriented perpendicularly to the applied mechanical deformation in the case of HDPE/wollastonite composites, indicating better polymer/filler adhesion in comparison to mica as highlighted in Figs. 2C and 2D by circles. It is known from the literature, that the orientation of the craze propagation is most clearly demonstrated in tensile tests on injection-molded bars, where crazes form readily in the interior of the bar. There, the polymer macromolecule orientation is low, and the crazes propagate outwards towards the surface, where the high orientation along the length of the bar brings them to a halt [41]. The alternative mechanism of deformation to shear yielding is craze formation, which is both a localized yielding process and the first stage of fracture. When a tensile stress is applied to a glassy polymer, small holes form in a plane perpendicular to the stress, to produce an incipient crack. However, the holes become stabilized by fibrils of oriented polymeric material which span the gap and prevent it from becoming wider. The resulting yielded region consisting of an interpenetrating network of voids and polymer fibrils, is known as a craze.

There was found a presence of the delamination of the mica filler from the surrounding matrix in the form of cavities in the case of the impact damage (Fig. 2E) indicating high mechanical energy dissipative capacity of the mica particles accompanied by the lance structure of the individually localized shearing bands.

A schematic representation of the general mechanical behavior observed under uniaxial tensile deformation testing is shown in Fig. 3. Here, there were found typical stress-strain patterns characteristic for the elastic region (I), elastic plastic transition region (II) and the stress plateau draw ratio region (III) in a similar fashion as in the case of calcium carbonate hollow spheres/HDPE composites [5]. However, in the case of HDPE/mica composites these exhibit typical stiff and brittle tensile deformation behavior, in contrary to the HDPE/wollastonite and neat HDPE samples which exhibited elasto-plastic mechanical behavior. It was found, that both fillers (wollastonite as well as mica) contribute to the increase of the Young´s modulus of elasticity *E* as shown in Fig. 4. The modulus *E* was increased by about 129 % for HDPE/mica composites and increased by 67 % for the HDPE/wollastonite composites. In absolute values the original HDPE *E* was (703 ± 73) MPa. With 15 w. % HDPE/mica the modulus of the composite was (1609 ± 93) MPa and for the HDPE/wollastonite composites the modulus was (1173 ± 107) MPa, as observed at the room temperature of 22°C and 50 mm/min deformation rate. The observed results confirmed well the known fact, that the stiff filler particles enhance the *E* of polymer based composites with increasing filler content in comparison to the virgin polymer matrix [43,44]. This behavior was ascribed to the higher crystallinity of the HDPE/mica polymer composites in comparison to HDPE/wollastonite composites (Table 1). Higher crystallinity polymers exhibit higher elastic properties rather than plastic, which is characteristic for amorphous polymeric systems [41]. As shown in Fig. 5, the observed upper yield fillers concentration dependencies exhibit mutually opposite linear behavior for each of the studied fillers: in the case of HDPE/mica

composites the observed trend is that the upper yield was increasing with increasing filler concentration for all tested deformation rates. For the deformation rate of 50 mm/min the upper yield was increased from (891 ± 20) MPa for virgin HDPE to (952 ± 27) MPa for HDPE/mica composites. This behavior was in agreement with data observed by Liang and Yang [45]. However, for HDPE/wollastonite composites the observed upper yield dependency decreased with increasing filler concentration to (855 ± 6) MPa. A similar behavior was obtained for all tested deformation rates. These results indicate the fact, that HDPE/mica composites have higher stiffness in comparison to HDPE/wollastonite composites. Fig. 6 shows results of the filler concentration strain at break dependencies measured at three different deformation rates. It is evident, that both the composites exhibited a linear decrease of strain at break with increasing filler concentrations for 100 mm/min and 200 mm/min deformation rates, indicating a more brittle mechanical behavior in comparison to the virgin HDPE polymer. However, the HDPE/wollastonite composites at 5 w.% filler concentration exhibited a 15 % increase in the magnitude of the strain at break (Fig. 6B) indicating an increase in ductility at 50 mm/min deformation rate. Observed dependency was modeled as a third order polynomial of the form of $y = 220.69 + 37.85\,x - 7.67\,x^2 + 0.29\,x^3$, where y is the strain at break (in %) and x is filler concentration (in w.%). For the 50 mm/min deformation rate of the HDPE/mica composites, the latter strain at break vs. concentration dependence (Fig. 6A) was modeled as $y = 220.69 - 25.23\,x + 1.32\,x^2 - 0.03\,x^3$. Strain rate has a complicated effect on materials deformation processes. The energy expended during plastic deformation is in majority dissipated as heat. However, this process was found to be more prominent at higher deformation rates associated with adiabatic drawing. At lower deformation rates the isothermal drawing was confirmed [10]. Fracture toughness measurements have shown, that the mineral fillers function as the stress concentrators in the polymer matrix which was reflected in the observed exponentially decreasing dependencies of

fracture toughness vs. filler concentration as shown in Fig. 7. It was found, that the HDPE/wollastonite composites exhibited higher toughness of about 12 % in comparison to the HDPE/mica composites. These findings were in excellent correlation with the uniaxial tensile testing results, confirming for both materials that increasing stiffness resulted in increasing Young´s modulus of elasticity (Fig. 4). The same conclusions were obtained for both composites from the mechanical vibration damping testing data, where it was confirmed the increasing material stiffness with increasing filler content as reflected by the shift of the first resonance frequency peak to higher excitation frequencies (Fig. 8). We assume our composite materials act as a spring-mass-damper mechanical system which is subjected to the base support harmonic motion excitation. As is known, due to the materials structural internal damping, the first resonance frequency of the base excited spring-mass-damper is always less than the undamped natural frequency which increases with the increasing stiffness of the system [38,45]. That is why, when in our case, the energy dissipative processes occur in the tested material system, e.g. due to the internal friction, the vibration energy damping increases as well. This is reflected in the lower material stiffness, hence observing a lower first resonance frequency of the transfer damping function. Furthermore, the natural frequency of the undamped system is proportional to the square root of the ratio of the material stiffness to the applied inertial mass. This leads to the decreasing dependence of the first resonance frequency with the increasing inertial mass for each of the studied filler concentrations (Fig. 8).

As mentioned above, due to the melt flow induced fillers spatial orientation in the injection molded testing articles, the fillers were oriented in the direction of their lowest hydrodynamic resistance. That is why, the steep increase of the first resonance frequency position for the 15 w. % HDPE/mica composites was ascribed to the effect of the proper pouring of the polymer macromolecular chains on the surface of the planar mica particles initiating stronger inter

particle as well as particle polymer interactions, enhancing the so-called confinement effects [11]. This phenomenon was not found for the HDPE/wollastonite composites. We assume that the prism shape high aspect ratio filler particles act as the stiffness increasing component, however, due to its elongated shape large volumes of the HDPE polymer matrix remained intact. As clearly demonstrated in results presented in Fig. 8 this mechanical behavior was evident only at the zero inertial mass transfer damping function measurements, with increasing inertial mass these results were not so pronounced, due to the restricted macromolecular chains motion resulting in higher matrix stiffness. This fact was confirmed also by the uniaxial tensile testing *E* modulus dependencies shown in Fig. 4. Here for the HDPE/mica composite the observed Young´s modulus filler concentration dependence increase was more intensive in comparison to HDPE/wollastonite composites. Results of the thermal analysis of the studied composites are shown in Table 1 and Fig. 9. It was found that with increasing filler concentration the crystallinity of the HDPE in HDPE/mica composites increased from 59 % for virgin HDPE to 77 % for 15 w. % HDPE/mica composite, indicating a positive effect of the mica nano-sheets planar crystalline facets on HDPE crystallization in a similar fashion as in the case of other planar filler materials such as clay [6,21]. The observed maximum thermal degradation rate of the HDPE/mica composites found was about 467 °C, which was in agreement with the earlier published data [46]. On the other hand, the crystallinity decreased from 62 % obtained for virgin HDPE to 56 % for the 15 w. % HDPE/wollastonite composites.

5. Conclusions

It was found in this study, that both fillers under study (mica and wollastonite) trigger an increase of Young´s modulus of elasticity with increasing filler concentration in HDPE composites. In the case of HDPE/mica the same increasing trend was found for the upper

yield point vs. filler concentration dependencies indicating higher material stiffness. However, for the HDPE/wollastonite composites this trend was reversed with a decrease of the upper yield point as well as of the strain at break. These findings were confirmed by mechanical vibration damping testing where there was a more intense shift of the first resonance frequency peak position to higher frequencies with increasing filler concentrations for HDPE/mica in comparison to HDPE/wollastonite composites. Both composites exhibited with increasing filler concentration a decreasing strain at break data, indicating a more brittle mechanical behavior of studied composites in comparison to the virgin HDPE polymer matrix. However, for HDPE/wollastonite composites at 5 w. % filler concentration a 15 % increase in the magnitude of the strain at break was found indicating an increase in ductility at 50 mm/min deformation rate. This phenomenon was not found for measurements at 100 and 200 mm/min deformation rates. Fracture toughness measurements show, that both studied fillers function as the stress concentrators in the HDPE polymer matrix, which was reflected in the observed exponentially decreasing dependencies of the fracture toughness vs. filler concentrations. It was found, that the HDPE/mica composites exhibited lower fracture toughness of about 12 % in comparison to the HDPE/wollastonite composites in the whole fillers concentration range tested. SEM analysis of the fracture surfaces show typical elongation bands of high plasticity deformation regions characterized with the typical shearing bands interpenetrated with cavities created around filler particles. Thermal analysis data showed for HDPE/mica composites a strong increase of the crystallinity with increasing filler concentration, however, in the case of HDPE/wollastonite composites an opposite effect of the higher amorphous polymer phase content was found.

Acknowledgements

Authors would like to express their gratitude to Ing. P. Zádrapa, Ph.D. for assistance with sample preparation. Partial financing of this research from the Ministry of Education, Youth and Sports of the Czech Republic (grant no. LO1305) and the Palacky University in Olomouc Internal Grant Agency (grant no. IGA_PrF_2017_028) is gratefully acknowledged.

References

[1] Vaia R. Adaptive and responsive polymer nanocomposites: Opportunities for smart materials. Proceedings of Eurofillers - A Conference on Functional Fillers for Shape Memory Advanced Applications, Zalakaros (Hungary) 2007.

[2] Liang J, Yang Q. Effects of carbon fiber content and size on electric conductive properties of reinforced high density polyethylene composites. Compos Pt B-Eng 2017;114:457-466.

[3] Savas LA, Tayfun U, Dogan M. The use of polyethylene copolymers as compatibilizers in carbon fiber reinforced high density polyethylene composites. Compos Pt B-Eng 2016;99:188-195.

[4] Erkendirci OF. Investigation of the quasi static penetration resistance behavior of carbon fiber reinforced laminate HDPE composites. Composites Part B-Engineering 2016;93:344-351.

[5] Lapcik L, Manas D, Vasina M, Lapcikova B, Reznicek M, Zadrapa P. High density poly(ethylene)/CaCO3 hollow spheres composites for technical applications. Compos Pt B-Eng 2017;113:218-224.

[6] Krasny I, Lapcik L, Lapcikova B, Greenwood RW, Safarova K, Rowson NA. The effect of low temperature air plasma treatment on physico-chemical properties of kaolinite/polyethylene composites. Composites Part B-Engineering 2014;59:293-299.

[7] Dasari A, Rohrmann J, Misra R. On the scratch deformation of micrometric wollastonite reinforced polypropylene composites. Mater Sci Eng A-Struct Mater Prop Microstruct Process 2004;364(1-2):357-369.

[8] Malik TM, Farooqi MI, Vachet C. Mechanical and Rheological Properties of Reinforced Polyethylene. Polym Compos 1992;13(3):174-178.

[9] Liang J-, Yang Q-. Mechanical, thermal, and flow properties of HDPE-mica composites. J Thermoplast Compos Mater 2007;20(2):225-236.

[10] Dasari A, Sarang S, Misra R. Strain rate sensitivity of homopolymer polypropylenes and micrometric wollastonite-filled polypropylene composites. Mater Sci Eng A-Struct Mater Prop Microstruct Process 2004;368(1-2):191-204.

[11] Kuelpmann A, Osman MA, Kocher L, Suter UW. Influence of platelet aspect ratio and orientation on the storage and loss moduli of HDPE-mica composites. Polymer 2005;46(2):523-530.

[12] Xiang Y, Hou Z, Su R, Wang K, Fu Q. The effect of shear on mechanical properties and orientation of HDPE/mica composites obtained via dynamic packing injection molding (DPIM). Polym Adv Technol 2010;21(1):48-54.

[13] Yim Y, Rhee KY, Park S. Electromagnetic interference shielding effectiveness of nickel-plated MWCNTs/high-density polyethylene composites. Compos Pt B-Eng 2016;98:120-125.

[14] Valente M, Tirillo J, Quitadamo A, Santulli C. Paper fiber filled polymer. Mechanical evaluation and interfaces modification. Compos Pt B-Eng 2017;110:520-529.

[15] Fernandes EM, Aroso IM, Mano JF, Covas JA, Reis RL. Functionalized cork-polymer composites (CPC) by reactive extrusion using suberin and lignin from cork as coupling agents. Composites Part B-Engineering 2014;67:371-380.

[16] Babaei I, Madanipour M, Farsi M, Farajpoor A. Physical and mechanical properties of foamed HDPE/wheat straw flour/nanoclay hybrid composite. Compos Pt B-Eng 2014;56:163-170.

[17] Singh R, Singh N, Fabbrocino F, Fraternali F, Ahuja IPS. Waste management by recycling of polymers with reinforcement of metal powder. Composites Part B-Engineering 2016;105:23-29.

[18] Grigoriadou I, Paraskevopoulos KM, Karavasili M, Karagiannis G, Vasileiou A, Bikiaris D. HDPE/Cu-nanofiber nanocomposites with enhanced mechanical and UV stability properties. Compos Pt B-Eng 2013;55:407-420.

[19] Cao Z, Daly M, Geever LM, Major I, Higginbotham CL, Devine DM. Synthesis and characterization of high density polyethylene/peat ash composites. Compos Pt B-Eng 2016;94:312-321.

[20] Zhu C, Zhang R, Huang Y, Yang W, Liu Z, Feng J, Yang M. Hierarchical crystalline structures induced by temperature profile in HDPE bars during melt penetration process. Chinese Journal of Polymer Science 2017;35(1):108-122.

[21] Singh VP, Vimal KK, Sharma S, Kapur GS, Choudhary V. Polyethylene/sepiolite clay nanocomposites: Effect of clay content, compatibilizer polarity, and molar mass on viscoelastic and dynamic mechanical properties. J Appl Polym Sci 2017;134(33):45197.

[22] Stuerzel M, Hees T, Enders M, Thomann Y, Blattmann H, Muelhaupt R. Nanostructured Polyethylene Reactor Blends with Tailored Trimodal Molar Mass Distributions as Melt-Processable All-Polymer Composites. Macromolecules 2016;49(21):8048-8060.

[23] Giboz J, Spoelstra AB, Portale G, Copponnex T, Meijer HEH, Peters GWM, Mele P. On the origin of the "core-free" morphology in microinjection-molded HDPE. Journal of Polymer Science Part B-Polymer Physics 2011;49(20):1470-1478.

[24] Jiang ZY, Tang YJ, Men YF. Morphological and structural evolution of tensile deformed high density polyethylene during melting: in situ synchrotron small-angle X-ray scattering study. Plastics Rubber and Composites 2010;39(9):392-399.

[25] Tarani E, Wurm A, Schick C, Bikiaris DN, Chrissafis K, Vourlias G. Effect of graphene nanoplatelets diameter on non-isothermal crystallization kinetics and melting behavior of high density polyethylene nanocomposites. Thermochimica Acta 2016;643:94-103.

[26] Abareshi M, Zebarjad SM, Goharshadi EK. Effect of milling time and clay content on the thermal stability of polyethylene-clay nanocomposite. Journal of Vinyl & Additive Technology 2016;22(3):285-292.

[27] Yang R, Liu Y, Yu J, Wang KH. Thermal oxidation products and kinetics of polyethylene composites. Polym Degrad Stab 2006;91(8):1651-1657.

[28] Plueddemann EP. Silane adhesion promoters. Coatings Technology Handbook, Second Edition 2001:563-565.

[29] Arkles B. Tailoring Surfaces with Silanes. Chemtech 1977;7(12):766-778.

[30] Plueddemann E, Stark G. Role of Coupling Agents in Surface Modification of Fillers. Modern Plast 1977;54(8):76-&.

[31] Zeltmann SE, Prakash KA, Doddamani M, Gupta N. Prediction of modulus at various strain rates from dynamic mechanical analysis data for polymer matrix composites. Compos Pt B-Eng 2017;120:27-34.

[32] Demange M. Mineralogy for petrologists optics, chemistry and occurrence of rock-forming minerals. CRC Press/Balkema, Leiden. 2012:182.

[33] Lapcik L, Vasina M, Lapcikova B, Otyepkova E, Waters KE. Investigation of advanced mica powder nanocomposite filler materials: Surface energy analysis, powder rheology and sound absorption performance. Composites Part B-Engineering 2015;77:304-310.

[34] Demidenko NI, Tel'nova GB. Microstructure and properties of a material based on natural wollastonite. Glass and Ceramics 2004;61(5-6):183-186.

[35] Dole M, Wunderlich B. The melting range of semicrystalline copolymers .2. J Polymer Sci 1957;24(105):139-143.

[36] Ahn Y, Jeon JH, Park J, Thenepalli T, Ahn JW, Han C. Effects of modified LDPE on physico-mechanical properties of HDPE/CaCO3 composites. Korean J Chem Eng 2016;33(11):3258-3266.

[37] Lapcik L, Vasina M, Lapcikova B, Valenta T. Study of bread staling by means of vibro-acoustic, tensile and thermal analysis techniques. J Food Eng 2016;178:31-38.

[38] Lapcik L, Vasina M, Lapcikova B, Plskova M, Gal R, Brychtova M. Application of a vibration damping technique in characterizing mechanical properties of chicken meat batters

modified with amaranth. Journal of Food Measurement and Characterization 2017;11(4):1987-1994.

[39] Bonfiglio P, Pompoli F, Horoshenkov KV, Rahim MIBSA. A simplified transfer matrix approach for the determination of the complex modulus of viscoelastic materials. Polym Test 2016;53:180-187.

[40] Pukanszky B, Vanes M, Maurer FHJ, Voros G. Micromechanical Deformations in Particulate Filled Thermoplastics - Volume Strain-Measurements. J Mater Sci 1994;29(9):2350-2358.

[41] Bucknall CB. Toughening of Plastics. Plastics & Rubber International 1978;3(5):211-211.

[42] Su J, Zhang J. Improvement of mechanical and dielectrical properties of ethylene propylene diene monomer (EPDM)/barium titanate (BaTiO3) by layered mica and graphite flakes. Composites Part B-Engineering 2017;112:148-157.

[43] Lapcik L, Jindrova P, Lapcikova B, Tamblyn R, Greenwood R, Rowson N. Effect of the talc filler content on the mechanical properties of polypropylene composites. J Appl Polym Sci 2008;110(5):2742-2747.

[44] Liang J, Yang Q. Mechanical, thermal, and flow properties of HDPE-mica composites. J Thermoplast Compos Mater 2007;20(2):225-236.

[45] Stephen NG. On energy harvesting from ambient vibration. J Sound Vibrat 2006;293(1-2):409-425.

[46] Oliveira PL, Araujo RS, Oliveira VR, Morais JS, Marques MdFV. Nanocomposites of Polyethylene Blends Using Organomica. Macromolecular Symposia 2016;367(1):143-150.

Figure headings

Figure 1. SEM images of the studied composites inorganic filler materials: A – mica (aspect ratio ~1.7), B – wollastonite (aspect ratio ~13.5).

Figure 2. SEM images of the fracture surfaces of the studied virgin HDPE, HDPE/mica and HDPE/wollastonite composite materials: A, B – HDPE/mica composites fracture surfaces after tensile testing (15 w.% mica concentration) at 50 mm/min deformation rate, C, D – HDPE/wollastonite composites fracture surfaces after tensile testing (15 w.% wollastonite concentration) at 50 mm/min deformation rate, E – HDPE/mica composite fracture surface after Charpy´s pendulum impact measurement, F – virgin HDPE fracture surface after Charpy´s pendulum impact measurement.

Figure 3. Stress vs. strain dependencies of tested composites samples as obtained for 50 mm/min deformation rates at ambient temperature. Filler concentration of 10 w. %.

Figure 4. Deformation rate dependencies of Young´s moduli vs. filler concentrations of HDPE composites. Filler materials: A – mica, B – wollastonite.

Figure 5. Deformation rate dependencies of upper yield vs. filler concentrations of HDPE composites. Filler materials: A – mica, B – wollastonite.

Figure 6. Deformation rates dependencies of strain at break vs. filler concentrations of HDPE composites. Filler materials: A – mica, B – wollastonite.

Figure 7. Fracture toughness and absorbed impact work vs. concentration dependences for HDPE mineral filler composites as observed by Charpy´s impact measurements: empty symbols – fracture toughness, full symbols – absorbed impact work.

Figure 8. Inertial mass dependencies of the first resonance frequencies vs. filler concentrations of HDPE composites. Filler materials: A – mica, B – wollastonite.

Figure 9. Thermal analysis results of the studied HDPE/mica and HDPE/wollastonite composites. Inset legend: filler concentrations.

Table headings

Table 1. Thermal analysis results of the studied HDPE/mica and HDPE/wollastonite composites.

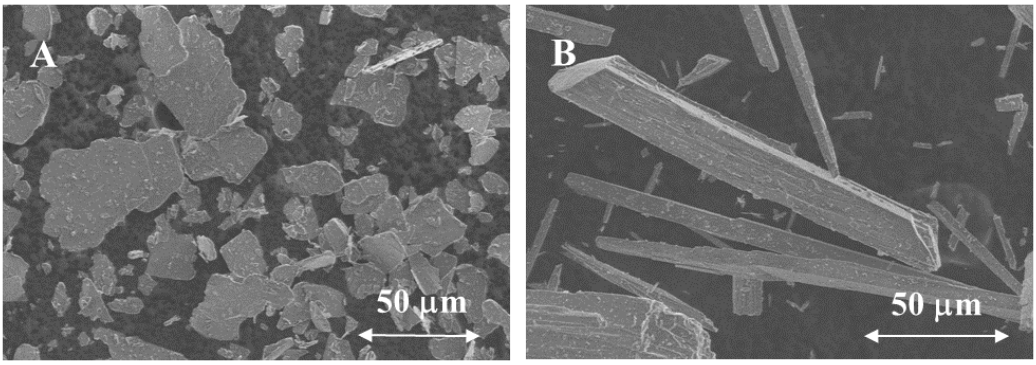

Fig. 1. SEM images of the studied composites inorganic filler materials: A – mica (aspect ratio 1.7), B – wollastonite (aspect ratio 13.5).

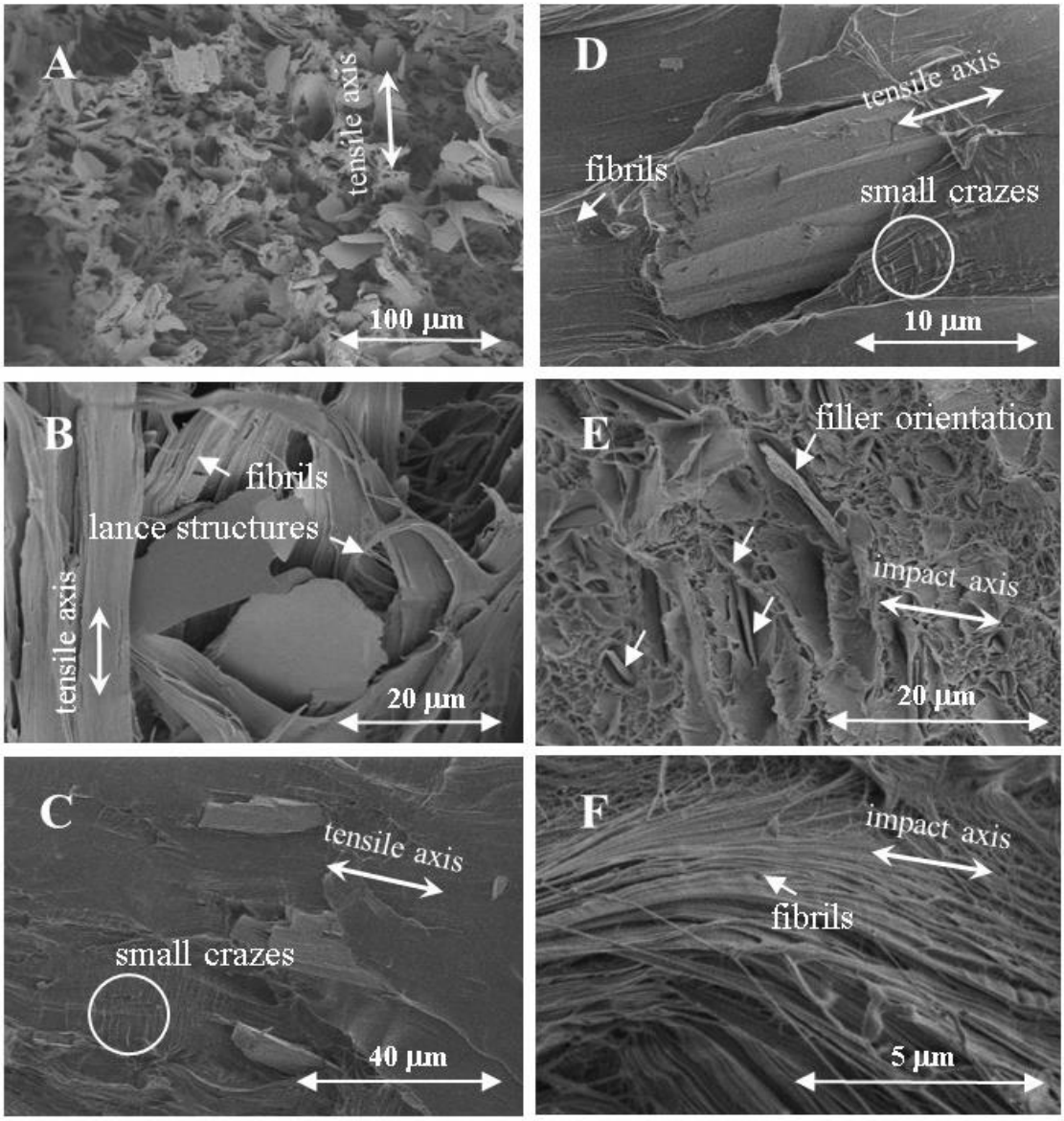

Fig. 2. SEM images of the fracture surfaces of the studied virgin HDPE, HDPE/mica and HDPE/wollastonite composite materials: A, B – HDPE/mica composites fracture surfaces after tensile testing (15 w.% mica concentration) at 50 mm/min deformation rate, C, D – HDPE/wollastonite composites fracture surfaces after tensile testing (15 w.% wollastonite concentration) at 50 mm/min deformation rate, E – HDPE/mica composite fracture surface after Charpy´s pendulum impact measurement, F – virgin HDPE fracture surface after Charpy´s pendulum impact measurement.

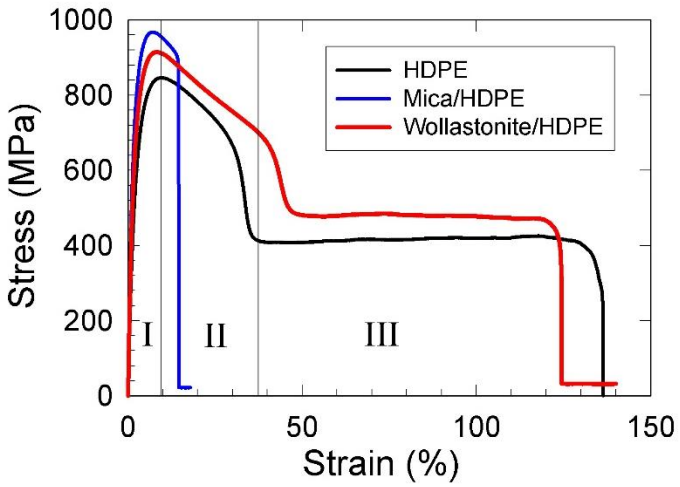

Fig. 3. Stress vs. strain dependencies of tested composites samples as obtained for 50 mm/min deformation rates at ambient temperature. Filler concentration of 10 w. %.

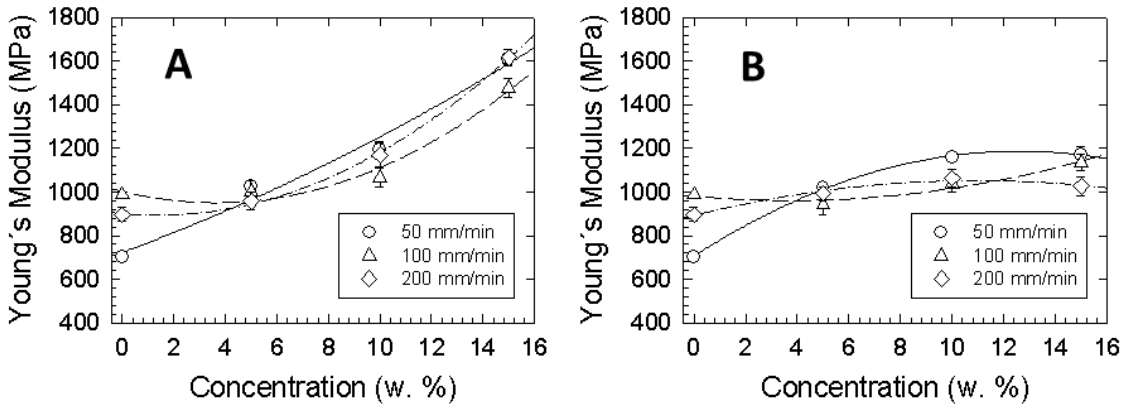

Fig. 4. Deformation rate dependencies of Young´s moduli vs filler concentrations of HDPE composites. Filler materials: A – mica, B – wollastonite.

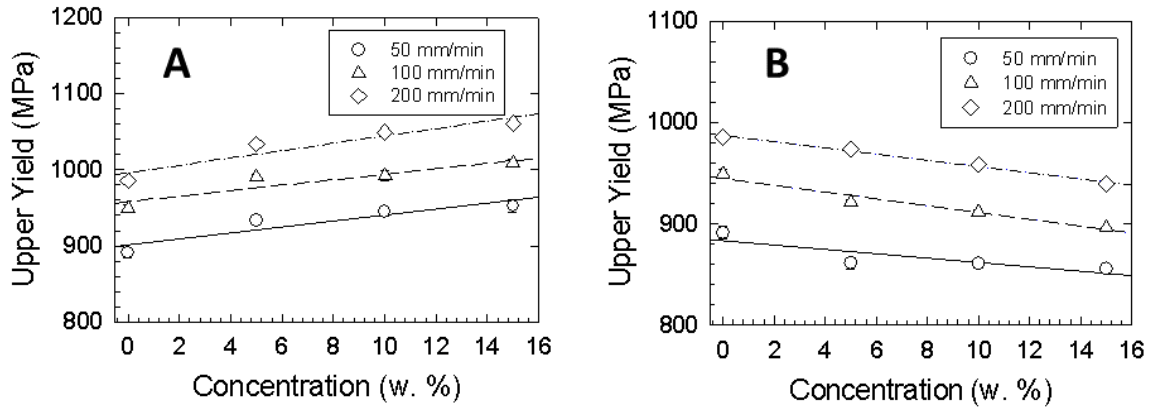

Fig. 5. Deformation rate dependencies of upper yield vs filler concentrations of HDPE composites. Filler materials: A – mica, B – wollastonite.

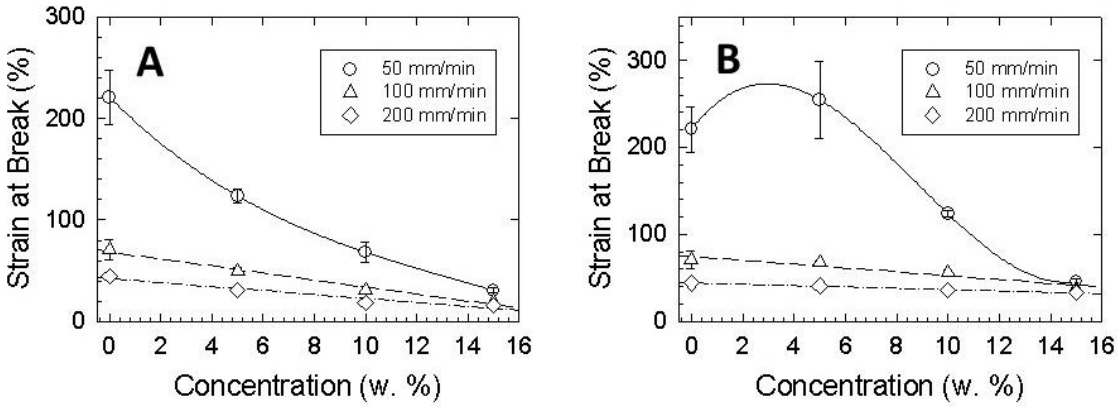

Fig. 6. Deformation rates dependencies of strain at break vs filler concentrations of HDPE composites. Filler materials: A – mica, B – wollastonite.

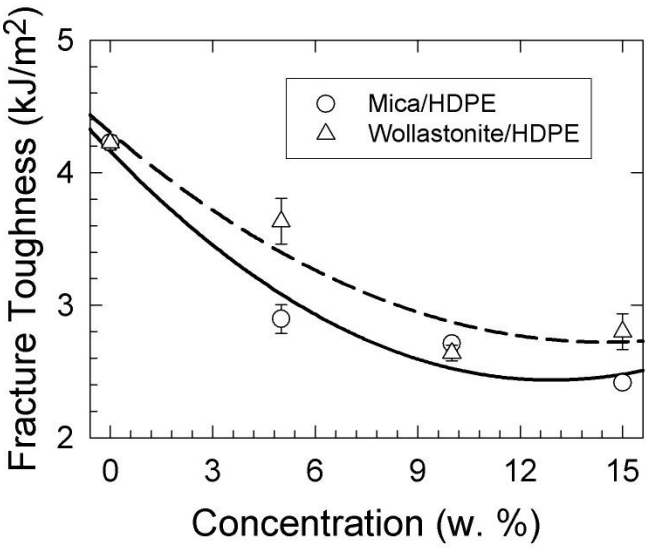

Fig. 7. Fracture toughness vs. concentration dependencies for HDPE mineral filler composites as observed by Charpy´s impact measurements.

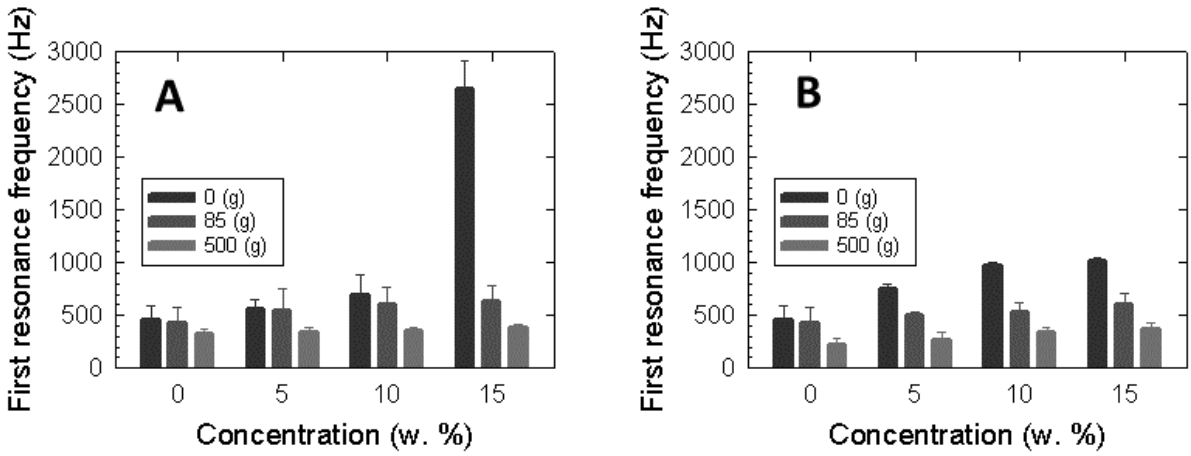

Fig. 8. Inertial mass dependencies of the first resonance frequencies vs filler concentrations of HDPE composites. Filler materials: A – mica, B – wollastonite.

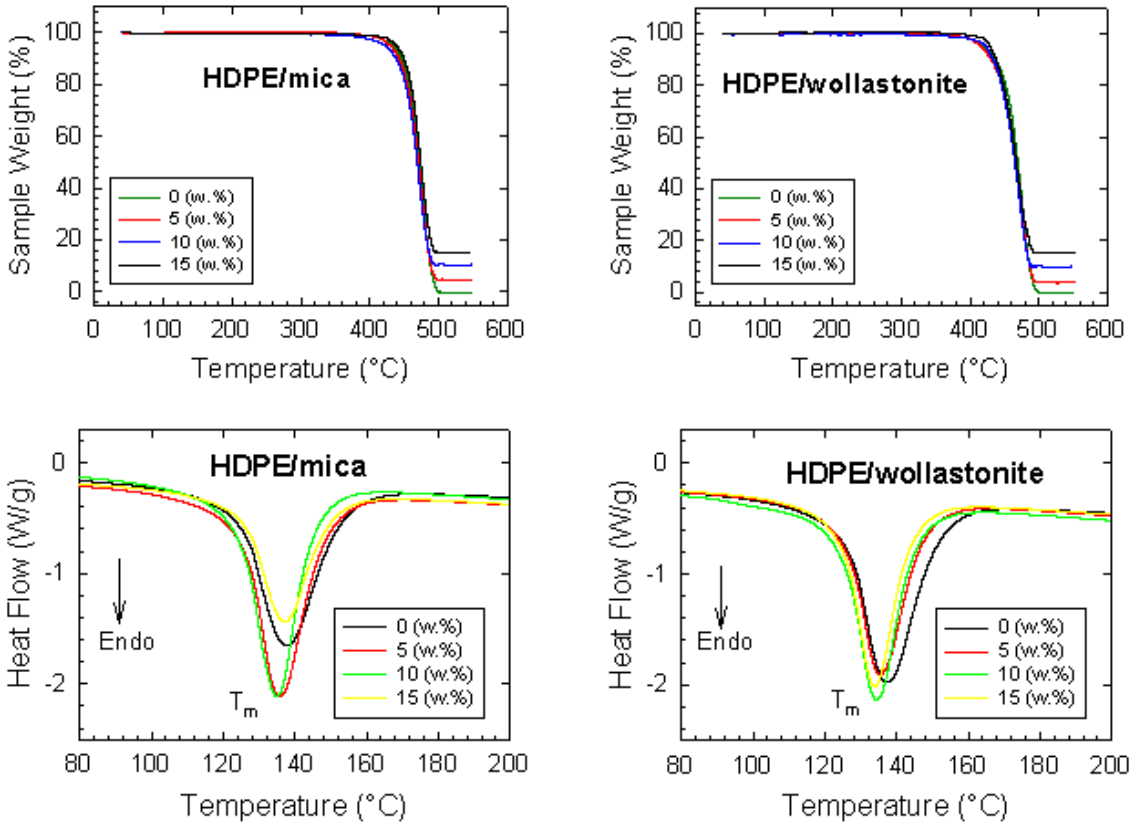

Fig. 9. Thermal analysis results of the studied HDPE/mica and HDPE/wollastonite composites. Inset legend: filler concentrations.

Table 1. Thermal analysis results of the studied HDPE/mica and HDPE/wollastonite composites.

c (w. %)	HDPE/mica			HDPE/wollastonite		
	T_m (°C)	ΔH_m (J/g)	X_C (%)	T_m (°C)	ΔH_m (J/g)	X_C (%)
0	137.67	172.42	58.85	137.39	182.20	62.18
5	135.72	183.15	65.80	135.41	146.13	52.50
10	135.02	172.95	65.59	134.46	162.02	61.44
15	134.90	190.89	76.65	133.81	139.24	55.91

c = filler concentration, T_m = melting temperature, ΔH_m = heat of fusion, X_C = crystallinity.